Vol. 8 (1) pp. 43-54, enero-junio del 2018
https://doi.org/10.21789/22561498.1373

RESEARCH ARTICLE

Effect of pH and Ttemperature on photocatalytic oxidation of methyl orange using black sand as photocatalyst

Efecto del pH y la temperatura sobre la oxidación fotocatalítica de naranja de metilo usando arena negra como fotocatalizador

Alejandra Ibatá Soto
Engineering Faculty, Environmental Engineering,
Universidad Libre, Colombia
https://orcid.org/0000-0001-6570-6547
alejandra.ibatas@unilibrebog.edu.co

Rafael Nikolay Agudelo Valencia
Engineering Faculty, Environmental Engineering,
Universidad Libre, Colombia
https://orcid.org/0000-0002-6646-7725
rafaeln.agudelov@unilibre.edu.co

Andrés Felipe López Vásquez
Department of Chemical Engineering,
Universidad Nacional de Colombia – sede Manizales, Colombia
https://orcid.org/0000-0002-6411-5494
aflopezv@unal.edu.co

Fecha de recepción: 2 de agosto del 2017
Fecha de aceptación: 7 de diciembre de 2017

Sugerencia de citación: Ibatá Soto, A., Agudelo Valencia, R. N., y López Vásquez, A. F. (2018). Effect of pH and Temperature on Photocatalytic Oxidation of Methyl Orange using Black Sand as Photocatalyst. *Mutis, 8*(1), 43-54, doi: http://dx.doi.org/10.21789/22561498.1373

Editor: Javier Hernández Fernández

ABSTRACT

Azo dyes are considered hazardous compounds for the environment and human health. Methyl orange is one type of azo dyes and it is widely used in textile, leather, and other chemical industries. The degradation of this compound is a challenge for traditional treatments. Advanced oxidation processes such as heterogeneous photocatalysis, sonolysis, radiolysis, etc., become an alternative for mineralizing organic compounds by producing a highly oxidant agent (OH•). Nowadays, a great number of research studies have tried to modify TiO_2 with metals in order to improve the degradation of hazardous pollutants such as azo dyes. This study used black sand as an alternative photocatalyst, evaluating the influence of pH (2, 5, 3 and 8) and temperature (20, 25, 30 and

35°C) on the photocatalytic oxidation of methyl orange. Black sand was magnetically separated. The fraction that showed the best characteristics for dye degradation was used. Experimental results allowed establishing that methyl orange photocatalytic oxidation is best performed at pH 2 and 30°C, with a degradation percentage of 96.93%. The reaction follows a pseudo-first order kinetic. In addition, the kinetic coefficient found at different temperatures was correlated using Arrhenius equation in order to determinate changes in the kinetic coefficient depending on the temperature. The equation pre-exponential coefficient was 374782115.1 and energy activation was -58,104.4 J mol^{-1} K^{-1}.

Keywords: Azo dyes, kinetic evaluation, heterogeneous photocatalysis, pH and temperature influence.

RESUMEN

Los colorantes azo son considerados compuestos peligrosos para el medio ambiente y la salud humana. Uno de estos compuestos es el naranja de metilo el cual ha sido ampliamente utilizado en industrias textiles, de cuero y otras industrias químicas. La degradación de este compuesto se ha convertido en un reto mediante tratamientos convencionales. Algunos procesos de oxidación avanzada como la fotocatálisis heterogénea, la sonólisis, la radiólisis, etc., constituyen una alternativa para la mineralización de compuestos orgánicos gracias a la generación in-situ de un radical altamente oxidante (OH•). En la actualidad, un gran número de investigaciones han tratado de modificar el TiO_2 con metales para mejorar la degradación de contaminantes peligrosos como los colorantes azo. En este estudio se utilizó arena negra como una alternativa de fotocatalizador para evaluar el efecto del pH (2,0, 5,8 y 8,0) y la temperatura (20, 25, 30 y 35 °C) en el proceso de oxidación fotocatalítica del naranja de metilo. Debido a las características del mineral, se aplicaron diferentes campos magnéticos para obtener fracciones que fueron utilizadas como semiconductor, de las cuales se utilizó la que exhibió mejores condiciones para la degradación del colorante. Los resultados experimentales permitieron determinar que la oxidación fotocatalítica de naranja de metilo presentó una mayor eficiencia con un pH 2.0 y a 30° C, con un porcentaje de degradación de 96.93 %. La reacción observada describió una cinética de pseudo primer orden y mediante la ecuación de Arrhenius se determinó el coeficiente cinético a diferentes temperaturas. El coeficiente pre exponencial de la ecuación fue de 374782115,1 y la energía de activación fue de -58104,4 J mol^{-1} K^{-1}.

Palabras clave: colorantes azo, evaluación cinética, fotocatálisis heterogénea, influencia del pH y la temperatura.

INTRODUCTION

Hazardous compounds such as azo dyes are known to be a major problem for the environment since their degradation process is not easily carried out by means of traditional treatments. Methyl orange (MO) is an azo dye considered as one of the main water pollutants (Figueroa, Vázquez & Alvarez-Gallegos, 2009; Hai, Yamamoto, Nakajima, & Fukushi, 2011; Martínez-Huitle & Brillas, 2009; Muda *et al*., 2010). Produced for textile, leather and pharmaceutical industries, the degradation of this compound cab be easily performed by reduction at cathode because of its positive high redox potential (Feng *et al*., 2009).

Photocatalytic processes have emerged with several advantages for organic wastewater treatment due to the complete destruction or mineralization of pollutants to carbon dioxide and inorganic constitutes in water and gas phases (Chen, Tsai & Huang, 2005; Wang, Zheng, Xu & Li, 2011). The main photocatalyst used in these processes is TiO_2 due to its low price, availability, non-photo-corrosion, suitable band gap energy and chemical stability (Haarstrick, Kut & Elmar, 1996; Matos, Laine & Herrmann, 2001). Nevertheless, the use of this semiconductor has presented some limitations for these treatments, considering the amount of energy required when using UV lamps or having a doped semiconductor with metals, such as gold (Cheng *et al*., 2016; Oros-Ruiz *et al*., 2012).

Heterogeneous catalysis on mineral surfaces is part of advanced oxidation processes and constitutes an alternative to degrade polluting compounds of water sources (Schoonen, Xu & Strongin, 1998), considering that this process stimulates the mineral activation

inside the visible spectrum of electromagnetic radiation and improves stability against photo-corrosion. The use of minerals as photocatalyst materials has been applied to the degradation of aromatic and phenolic compounds (Sonawane & Dongare, 2006) and oxalic acid (Iliev *et al*., 2006), among others, with relatively satisfactory results (Arshadi *et al*., 2016).

The use of the mineral conglomerate known in this study as black sand (BS) has not been a common practice in this type of studies. In contrast, this material has been widely used in applications in the field of metallurgy. BS is composed by iron oxides, calcium, magnesium and silicon (Vargas & Forero, 2011), whose properties foster its use as a photocatalyst. A previous study showed that the magnetic separation of BS recovered from Colombian beaches (Santa Marta), named M1, M2, NM (Non-magnetic) and RM (raw material), was highly effective, showing higher discoloration percentages in MO compared to raw materials (Acosta, Ibatá & López, 2016). The most effective fraction was M2, which was exposed to a magnetic field of 0.1645 T. Therefore, pH influence in the solution is a variable to consider, since it affects dyes' absorption capacity, absorbent surface and solubility. It is important to emphasize that the discoloration process of MO works better at acid pH, and decreases its efficacy at alkaline pH. This because the absorbent surface increases its positive charge with acid pH and MO molecules reach its maximum positive charge, favoring electrostatic absorption (Subbaiah & Kim, 2016).

The effectiveness and speed of every chemical reaction is directly influenced by temperature (Lien & Zhang, 2007). As an example, high temperatures can accelerate the speed of MO molecules, possibly leading to an increase in absorption efficiency. However, when temperature exceeds 65°C efficiency decreases as a result of a week intermolecular attraction of absorbent materials (Arshadi *et al*., 2016). Previous studies about MO degradation have shown that kinetic degradation of MO is described by a pseudo-first model (Lee *et al*., 2015; Li, Li, Li & Yin, 2006; Yan *et al*., 2016). In that sense, this study is carried out in order to find optimum conditions for the photocatalytic oxidation process of MO using BS as semiconductor and pH and temperature as process variables. In addition, we study the kinetic tendency of MO degradation at different temperatures.

MATERIALS AND METHODS

Material Black Sand

The material was separated in four fractions by magnetic fields in order to make the best use of its high iron content, as suggested in a previous study (Acosta, Ibatá & López, 2016). The fraction that was used (M2) in the experimental phase was magnetically separated by a magnetic field of 0.164T; this fraction was used because of its composition. M2 fraction was evaluated to identify its chemical (XRF), morphological (SEM micrographs) and structural (XRD) characterization. Additionally, an EDX analysis was carried out with the purpose of determining its elemental composition.

Photocatalytic oxidation of methyl orange

M2 fraction was evaluated through the photocatalytic oxidation of 150 mL of MO to 20 mg L^{-1} in aqueous suspension with a BS dosage of 1.0 g L^{-1}. This reaction was carried out in an immersed well quartz photoreactor (Ace Glass Inc.) equipped with a cooling tube. Besides, 10 mmol of H_2O_2 were added to improve the photocatalytic activity of the mineral (Gao, Yang, Hu & Zhang, 2004; He *et al*., 2015; Sahel *et al*., 2016). In order to study the effect of the initial pH solution, the value was adjusted by adding of HCl and/or NaOH solutions. For these case, were tested at pH 2.0, MO natural pH (5.8) and 8.0. The experiments were carried out at 20, 25, 30 and 35°C. Reactions were carried out during three hours under UV-Vis irradiation (λ=310 nm) in magnetic stirring with 30 minutes of non-illumination, in order to reach adsorption-desorption equilibrium. MO samples were withdrawn from the reactor with a semiconductor, which was in turn removed from the liquid phase by thermo scientific centrifuge. Kinetic degradation of MO samples was evaluated by measuring MO signal disappearance every 30 minutes with a UV-Vis Shimadzu 2600 spectrophotometer. An evaluation of kinetic degradation for each reaction was performed using the coefficient of degradation as a way to determine the treatment with the highest speed reaction. The concentration of the substrate was measured at the beginning (C_o) and end of the treatment (C_f).

Table 1. Description of treatment conditions under different pH levels for MO photocatalytic oxidation.

Fraction	pH	Wavelength (nm)
M2	2.0	506
M2	5.3 (MO pH)	464
M2	8.0	464

RESULTS AND DISCUSSION

Chemical characterization of M2 fraction

The results obtained through X-ray fluorescence analysis showed that the mineral presents a representative percentage of iron oxides such as Fe_2O_3 (50.313 %w/w), with a slight difference with the percentage of TiO_2 (37.027 %w/w) (G.A. Reyes Gomez, 2015). Figure 1 shows the results of X-ray energy dispersive analysis (VEGA3 TESCAN) for the elemental composition by weight percent of M2 fraction (used as semiconductor for photocatalytic experiments), which it is mainly composed by iron (32.89%), titanium (26.74%), aluminium (1.18%) and oxygen (39.67%). The high amount of iron in the sample could be the main reason of the discoloration of MO, since iron could help doping TiO_2 naturally, improving its photocatalytic activity.

Figure 1. EDX analysis of black sand (M2 fraction) used as semiconductor during MO photocatalytic oxidation.

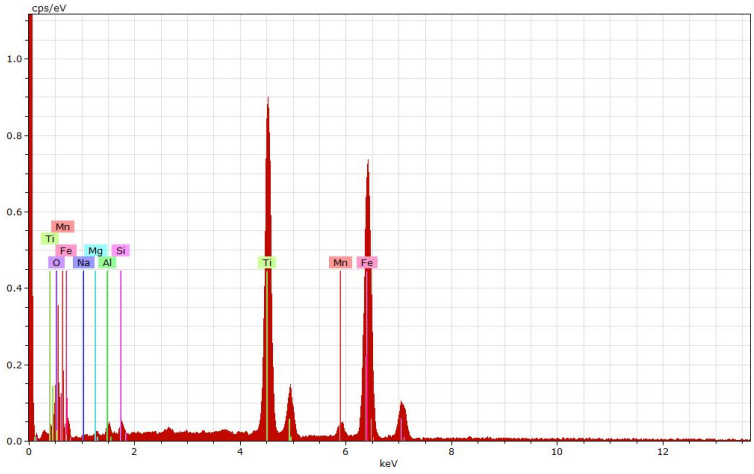

Source: Own elaboration.

Morphological and structural characterization of M2 fraction

In order to determinate the morphological structure of M2 fraction, we carried out an analysis with scanning electron microscopy (VEGA3 TESCAN), which showed that the mineral fraction is composed by irregular, rounded and semi-rounded grains (Figure 2).

X-ray diffraction analysis (X-ray powder diffractometer PANalytical X'Pert Pro PW 3064/60) with Cu-Kα radiation, was carried out to evaluate the crystalline phases of M2 fraction (Figure 3). This fraction was characterised for its content of iron oxides in the form of magnetite Fe_3O_4 (~ 99.0 %), showing a few amount of zircon, pyroxenes, altered grains and silicates (such as quartz), that might help improve the photocatalytic mechanism for MO photocatalytic oxidation.

MO photocatalytic oxidation

MO photocatalytic oxidation experiments were carried out with two process variables (pH and temperature), while the response variable was the removal percentage of MO.

Figure 2. Micrographs SEM of black sand (M2 fraction) used as semiconductor during MO photocatalytic oxidation.

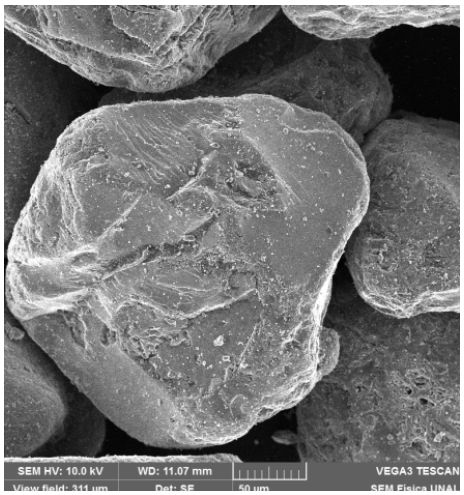

Source: Reyes Gomez, G.A. (2015).

Figure 3. XRD analysis of black sand (M2 fraction) used as semiconductor during MO photocatalytic oxidation.

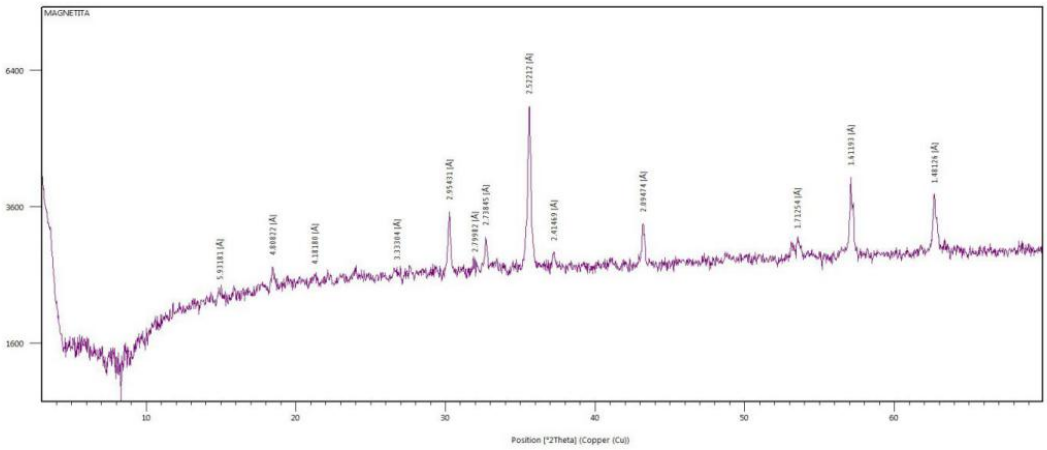

Source: Own elaboration.

Influence of pH

Table 2 shows the results of initial and final conditions of each experiment.

The absorption capacity of materials decreases when the pH of the solution increases, which means that the absorption process is possibly carried out with high effectiveness to acid pH, thus increasing the efficiency of the material (Subbaiah & Kim, 2016). Figure 4 (a-b) shown the UV-Vis spectra for the photocatalytic oxidation of MO as a time function. At the beginning of the reaction, the degradation showed a higher

Table 2. Discoloration percentage according to the pH evaluated.

pH	Absorbance (u.a)		Discoloration percentage (%)	Wavelength (nm)
	Initial	Final		
2.0	2.392	0.208	91.22	506
5.3	1.431	1.303	8.94	464
8.0	1.476	1.292	11.47	464

Source: Own elaboration.

speed than at the end. Nonetheless, it is possible to state it is necessary to allow the reaction time up to 180 min (or even more) in order to obtain the highest possible discoloration of MO. On the contrary, when pH increases, the photocatalytic oxidation of MO is less effective (Figure 4c-4f). This means that the MO photocatalytic oxidation was favored at acid conditions, while at alkaline conditions, the process is governed by hydrolysis (Arshadi *et al*., 2016; Dagar & Narula, 2016).

Figure 4. UV-Vis spectra of MO as a function on time at pH 2.0 (a-b), pH 5.3 (c-d) and pH 8.0 (e-f).

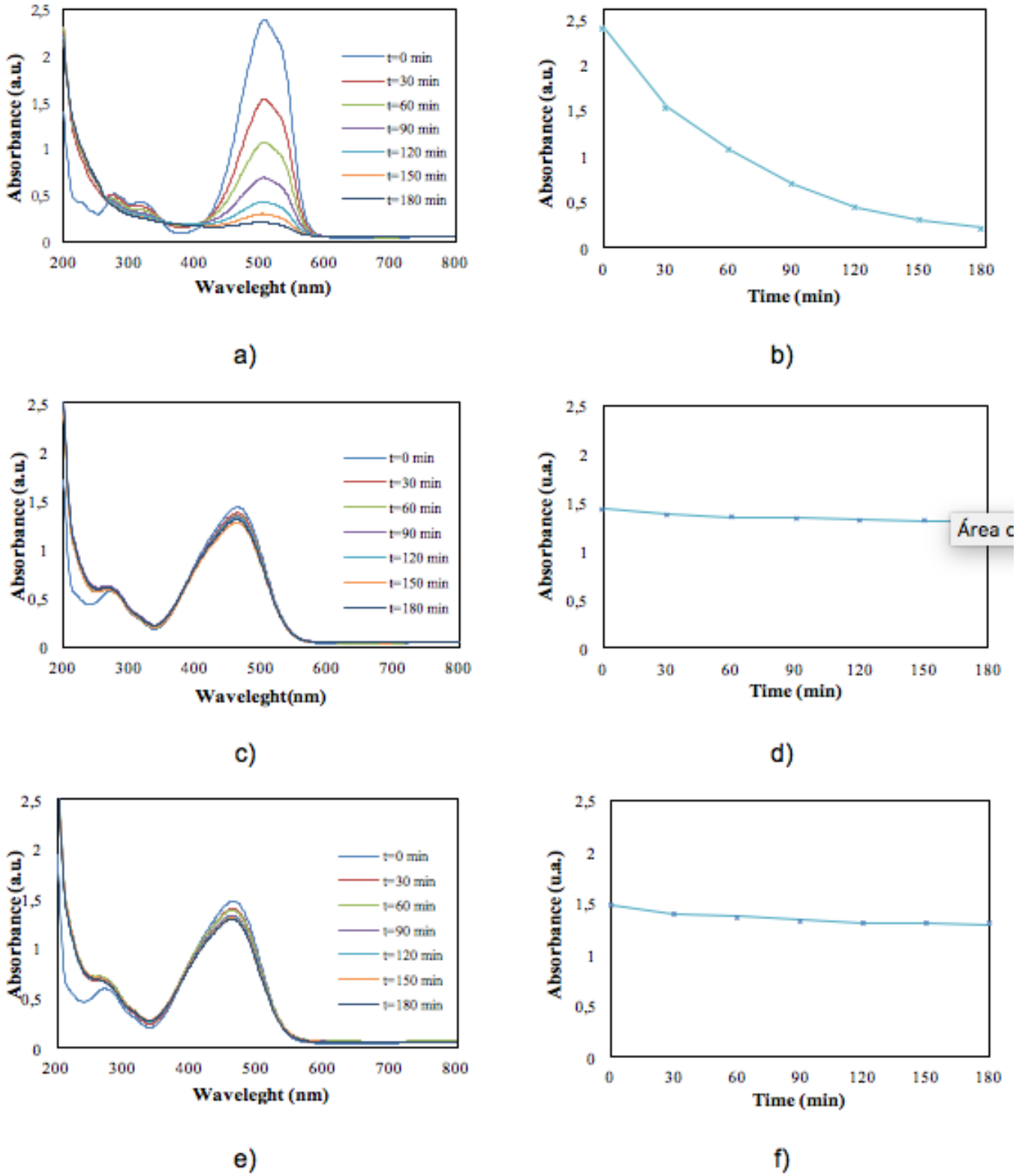

Influence of temperature

Once the optimal pH condition for mo photocatalytic oxidation was determined, the effect of temperature of solution was tested. According to literature, this process is more efficient when temperature does not exceed 65°C. On the other hand, H2O2 is thermally decomposed into oxygen and water at higher temperature, eventually scavenging the production of reactive radicals (Herney-Ramirez, Vicente & Madeira, 2010) however, the reaction is less efficient when temperature is below 25°C (Arshadi et al., 2016).

Figure 5 shows the mo photocatalytic degradation as function of solution temperature. A slight discoloration percentage can be appreciate with the temperature increase however, this maximum can be obtained at less time reaction (Figure 5e-f)

About concentration, mo photocatalytic oxidation exhibits several profiles of discoloration, reaching maximum values at different temperatures promoting a reduction in the reaction time, decreasing the operational costs in the process, especially in energy consumption for irradiation.

Figure 5. UV-Vis spectra and MO concentration during MO photocatalytic oxidation as a function on time at several temperatures. (a, b). 20ºC (c, d) 25ºC (e, f). 30ºC (g, h) 35ºC.

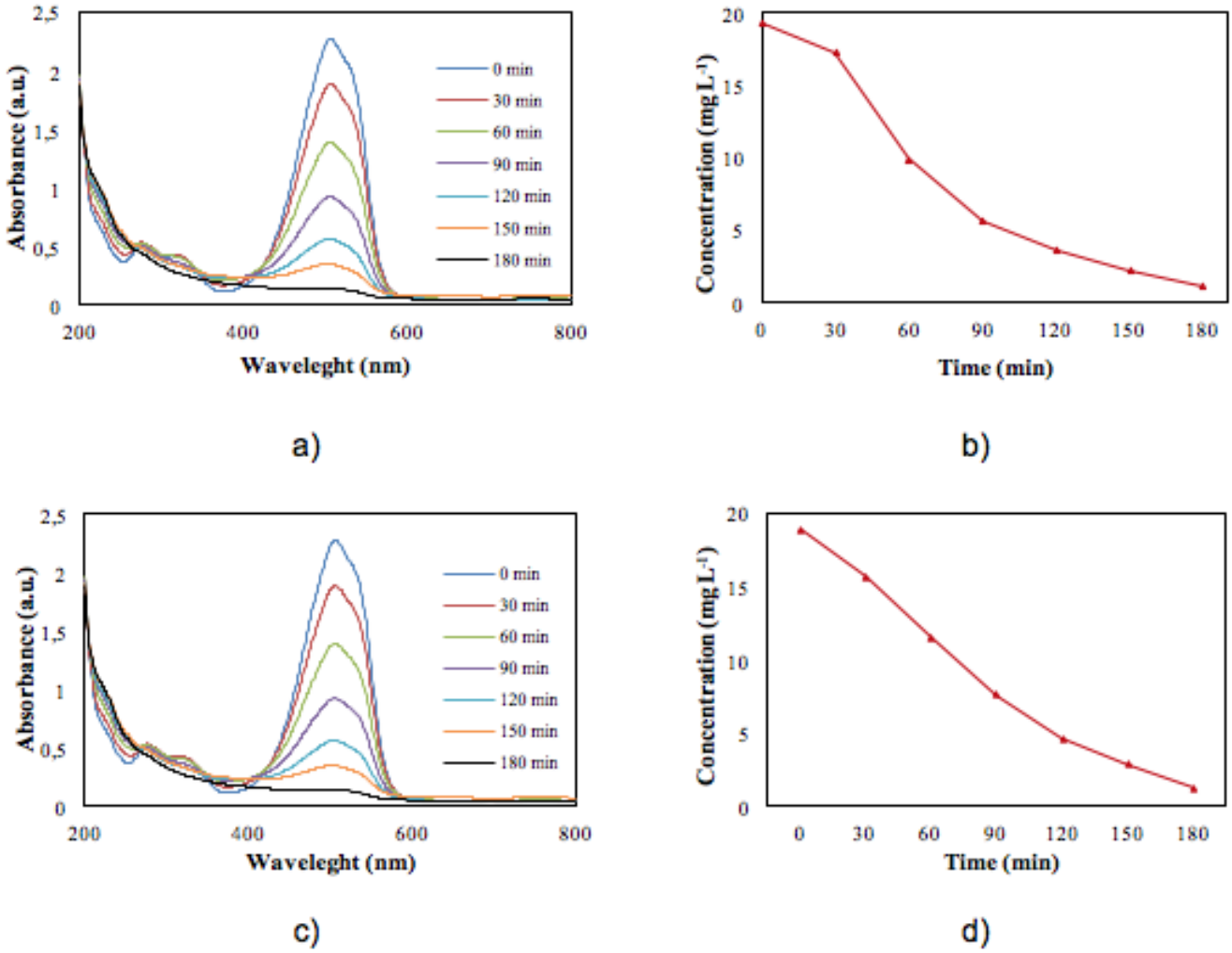

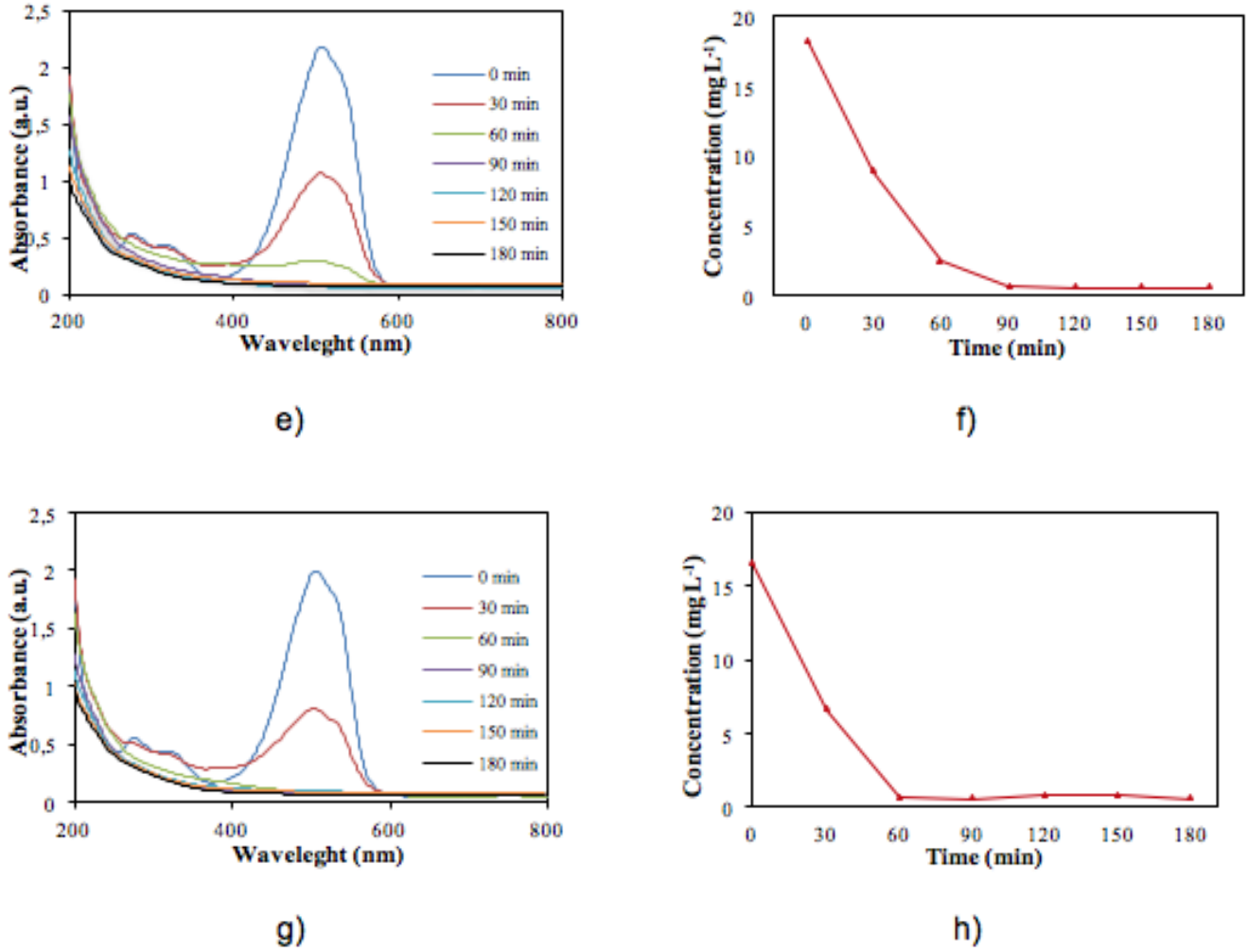

Source: Own elaboration.

Kinetic studies for MO photocatalytic oxidation at different temperatures

MO photocatalytic oxidation data were adjusted at pseudo-first order kinetic model. This goes in line with results of previous research studies on the subject (Lee *et al*., 2015; Matouq *et al*., 2014). The lineal correlation of the results was performed in order to calculate the kinetic coefficients K_{app} of the reactions at different temperatures, according to Eq. 1 (Dagar & Narula, 2016).

$$-\frac{dC}{dt} = K_{app} * C \quad (1)$$

The linearized form (Eq. 2) produces

$$Ln\left(\frac{C}{C_o}\right) = -K_{app} * t \quad (2)$$

where K_{app} is the slope of the graph, *y* axis is the natural logarithm of the quotient between the final and initial concentration, and *x* axis is the reaction time.

Figure 6 shows the linearized form of the kinetic data analysed. When temperature increased, the stable condition was reached in less time. The highest removal percentage was reached at 30°C. A slight decrease in the effectiveness of the reaction for MO degradation was observed at 35°C. As mentioned, the values used to construct the graphs were correlated to establish the value of the kinetic coefficient.

Figure 6. Degradation kinetics of the reaction at 20ºC (a), 25ºC (b), 30ºC (c) and 35ºC (d).

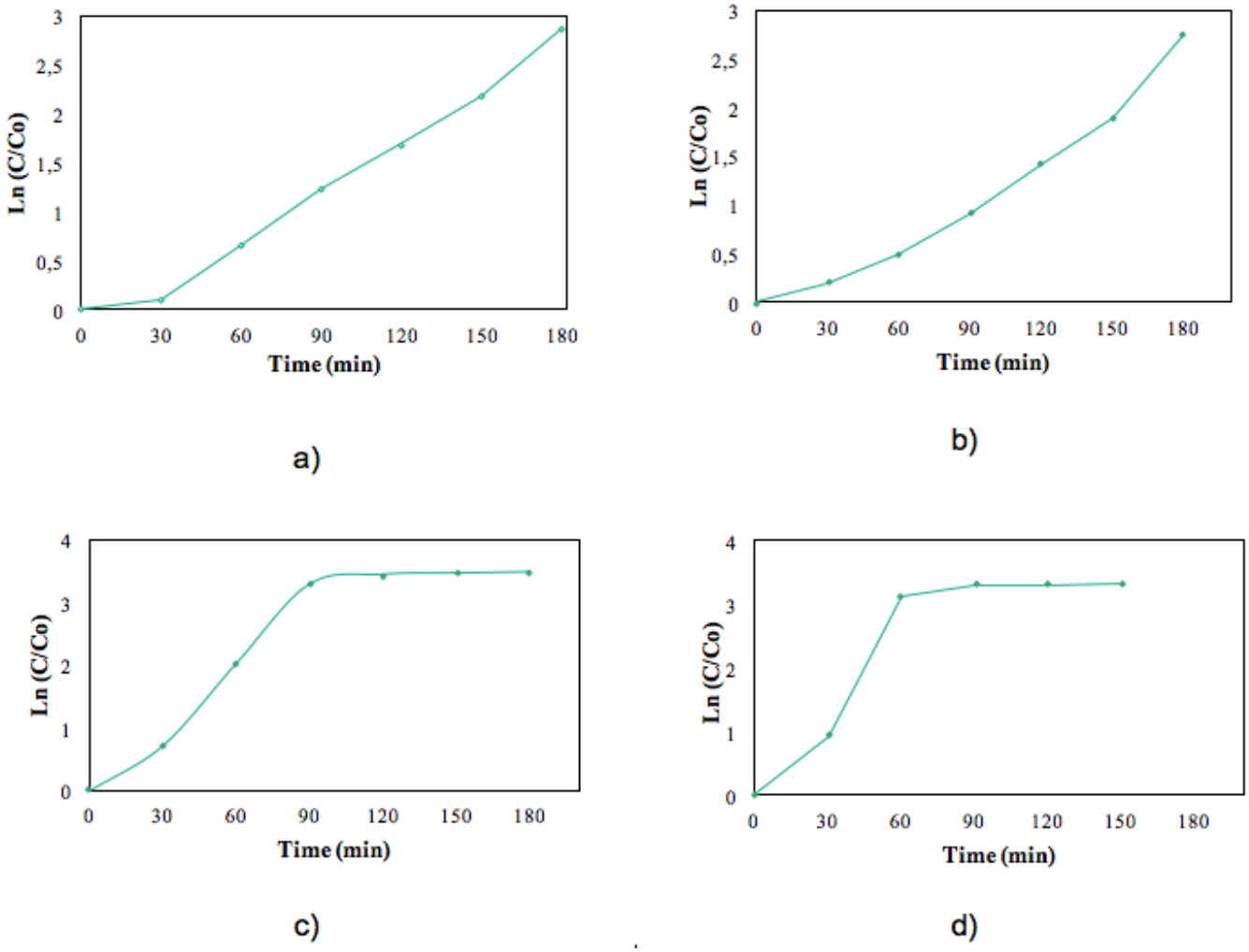

Source: Own elaboration.

Table 3 presents the values of the coefficients calculated at different temperatures, which increases with temperature solution. Once kinetics coefficients and temperature were identified, we calculated the variation of the kinetic coefficient with the temperature using Svante Arrhenius equation (Dahm & L. Brezonik, 1995), whose linearized form is represented by Eq. 3.

$$Ln\,(K) = Ln\,A - \frac{E_a}{R * T} \quad (3)$$

where E_a is the activation energy (J mol^{-1}), A the pre-exponential factor of Arrhenius, R the gas constant (8,314472 J mol^{-1} K^{-1}), and T is temperature (K). Figure 7 shown the linearization of (3) for the determination of kinetic constants.

Table 3. Correlation of the values to determine kinetic coefficients of reactions.

Temperature (°C)	Kinetic coefficient (min^{-1})	Correlation
20	0.016	0.983
25	0.025	0.958
30	0.037	0.985
35	0.052	0.946

Source: Own elaboration.

Figure 7. Linearized form of the Arrhenius equation to determine the activation energy of the reaction.

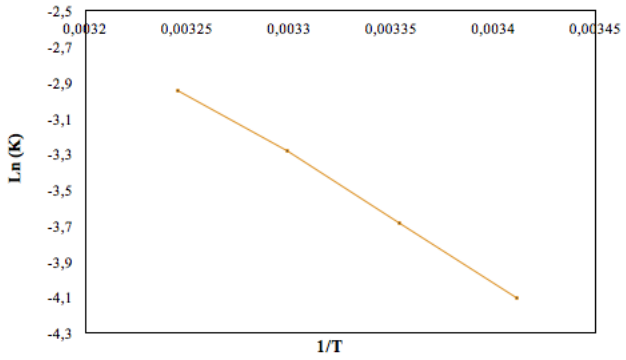

Source: Own elaboration.

The value obtained for the activation energy of MO degradation was -58104.41 J mol^{-1}. The pre exponential coefficient was 374782115.1 min^{-1}, with a statistical correlation coefficient of R^2 0.998. Finally, Eq. 4 allows calculating the kinetic coefficient as a function on temperature for MO photocatalytic oxidation

$$K_T = 374782115.1 \times e^{\frac{-58104.41 J\ mol^{-1}}{8.314472\ J\ mol^{-1} K^1 \times T}} \quad (4)$$

CONCLUSIONS

Results of the activation energy determined MO photocatalytic oxidation. It is concluded that BS could be used as an alternative semiconductor with better economic benefits for the degradation process of organic compounds, compared with the activation energy using TiO_2 as semiconductor (44.1 kJ mol^{-1}) (Arshadi *et al*., 2016). These results allow concluding that optimal conditions for higher removal efficiency of MO (96.93%) under UV irradiation are: 1.0 g L^{-1} dosage of BS, pH 2 and 30°C, with a reaction time of 90 min. It is important to mention that at 35°C the reaction time was 60 min, with a slightly higher removal percentage (96.339%).

REFERENCES

Acosta, P., Ibatá, A., & López, A. (2016). Evaluation of the Discoloration of Methyl Orange Using Black Sand as Semiconductor through Photocatalytic Oxidation and Reduction. *International Scholarly and Scientific Research & Innovation*, *10*(10), 1349-1353.

Arshadi, M., Abdolmaleki, M. K., Mousavinia, F., Khalafi-Nezhad, A., Firouzabadi, H., & Gil, A. (2016). Degradation of methyl orange by heterogeneous Fenton-like oxidation on a nano-organometallic compound in the presence of multi-walled carbon nanotubes. *Chemical Engineering Research and Design*, *112*(Supplement C), 113-121. doi:10.1016/j.cherd.2016.05.028.

Chen, L. C., Tsai, F. R., & Huang, C. M. (2005). Photocatalytic decolorization of methyl orange in aqueous medium of TiO2 and Ag–TiO2 immobilized on γ-Al2O3. *Journal of Photochemistry and Photobiology A: Chemistry*, *170*(1), 7-14. doi:10.1016/j.jphotochem.2004.07.012.

Cheng, X. Q., Ma, C. Y., Yi, X. Y., Yuan, F., Xie, Y., Hu, J. M., … & Zhang, Q. Y. (2016). Structural, morphological, optical and photocatalytic properties of Gd-doped TiO2 films. *Thin Solid Films*, *615*(Supplement C), 13-18. doi:10.1016/j.tsf.2016.06.049.

Dagar, A., & Narula, A. K. (2016). Photo-degradation of methyl orange under visible light by PEDOT/NiO/Fly ash cenosphere. *Materials Chemistry and Physics*, *183*(Supplement C), 561-570. doi:10.1016/j.matchemphys.2016.09.015.

Dahm, C., & L. Brezonik, P. (1995). Chemical Kinetics and Process Dynamics in Aquatic Systems. *Journal of the North American Benthological Society*, *14*, 354.

Feng, C., Liu, L., Li, F., & Li, X. (2009). Microbial fuel cell with an azo-dye-feeding cathode. *Applied Microbiology and Biotechnology*, *85*, 175-183.

Figueroa, S., Vázquez, L., & Alvarez-Gallegos, A. (2009). Decolorizing textile wastewater with Fenton's reagent electrogenerated with a solar photovoltaic cell. *Water Research*, *43*(2), 283-294. doi:10.1016/j.watres.2008.10.014.

Gao, Y., Yang, M., Hu, J., & Zhang, Y. (2004). Fenton's process for simultaneous removal of TOC and Fe2+ from acidic waste liquor. *Desalination*, *160*, 123-130.

Hai, F. I., Yamamoto, K., Nakajima, F., & Fukushi, K. (2011). Bioaugmented membrane bioreactor (MBR) with a GAC-packed zone for high rate textile wastewater treatment. *Water Research*, *45*(6), 2199-2206. doi:10.1016/j.watres.2011.01.013.

He, H., Zhong, Y., Liang, X., Tan, W., Zhu, J., & Wang, C. Y. (n.d.). Natural Magnetite : an efficient catalyst for the degradation of organic contaminant. *Nature Publishing Group*, 1-10.

Herney-Ramirez, J., Vicente, M. A., & Madeira, L. M. (2010). Heterogeneous photo-Fenton oxidation with pillared clay-based catalysts for wastewater treatment: A review. *Applied Catalysis B: Environmental*, *98*(1), 10-26. doi:10.1016/j.apcatb.2010.05.004.

Iliev, V., Tomova, D., Todorovska, R., Oliver, D., Petrov, L., Todorovsky, D., & Uzunova-Bujnova, M. (2006). Photocatalytic properties of TiO2 modified with gold nanoparticles in the degradation of oxalic acid in aqueous solution. *Applied Catalysis A: General*, *313*(2), 115-121. doi:10.1016/j.apcata.2006.06.039.

Lee, H. J., Kim, J. H., Park, S. S., Hong, S. S., & Lee, G. D. (2015). Degradation kinetics for photocatalytic reaction of methyl orange over Al-doped ZnO nanoparticles. *Journal of Industrial and Engineering Chemistry*, *25*(Supplement C), 199-206. doi:10.1016/j.jiec.2014.10.035.

Li, Y., Li, X., Li, J., & Yin, J. (2006). Photocatalytic degradation of methyl orange by TiO2-coated activated carbon and kinetic study. *Water Research*, *40*(6), 1119-1126. doi:10.1016/j.watres.2005.12.042.

Lien, H. L., & Zhang, W. X. (2007). Nanoscale Pd/Fe bimetallic particles: Catalytic effects of palladium on hydrodechlorination. *Applied Catalysis B: Environmental*, *77*(1), 110-116. doi:10.1016/j.apcatb.2007.07.014.

Martínez-Huitle, C. A., & Brillas, E. (2009). Decontamination of wastewaters containing synthetic organic dyes by electrochemical methods: A general review. *Applied Catalysis B: Environmental*, *87*(3), 105-145. doi:10.1016/j.apcatb.2008.09.017.

Matos, J., Laine, J., & Herrmann, J. M. (2001). Effect of the Type of Activated Carbons on the Photocatalytic Degradation of Aqueous Organic Pollutants by UV-Irradiated Titania. *Journal of Catalysis*, *200*(1), 10-20. doi:10.1006/jcat.2001.3191.

Matouq, M., Al-Anber, Z., Susumu, N., Tagawa, T., & Karapanagioti, H. (2014). The kinetic of dyes degradation resulted from food industry in wastewater using high frequency of ultrasound. *Separation and Purification Technology*, *135*(Supplement C), 42-47. doi: 10.1016/j.seppur.2014.08.002

Muda, K., Aris, A., Salim, M. R., Ibrahim, Z., Yahya, A., van-Loosdrecht, M. C. M., … & Nawahwi, M. Z. (2010). Development of granular sludge for textile wastewater treatment. *Water Research*, *44*(15), 4341-4350. doi:10.1016/j.watres.2010.05.023.

Oros-Ruiz, S., Gómez, R., López, R., Hernández-Gordillo, A., Pedraza-Avella, J. A., Moctezuma, E., & Pérez, E. (2012). Photocatalytic reduction of methyl orange on Au/TiO2 semiconductors. *Catalysis Communications*, *21*(Supplement C), 72-76. doi:10.1016/j.catcom.2012.01.028.

Reyes Gomez, G.A. (2015). Producción fotocatalítica de hidrógeno basada en el mineral arena negra, Universidad Libre sede Principal, https://repository.unilibre.edu.co/handle/10901/9974?show=full.

Sahel, K., Elsellami, L., Mirali, I., Dappozze, F., Bouhent, M., & Guillard, C. (2016). Hydrogen peroxide and photocatalysis. *Applied Catalysis B: Environmental*, *188*(Supplement C), 106-112. doi:10.1016/j.apcatb.2015.12.044.

Schoonen, M. A. A., Xu, Y., & Strongin, D. R. (1998). An introduction to geocatalysis. *Journal of*

Geochemical Exploration, *62*(1), 201-215. doi:10.1016/S0375-6742(97)00069-1.

Sonawane, R. S., & Dongare, M. K. (2006). Sol-gel synthesis of Au/TiO2 thin films for photocatalytic degradation of phenol in sunlight. *Journal of Molecular Catalysis A: Chemical*, *243*(1), 68-76. doi:10.1016/j.molcata.2005.07.043.

Subbaiah, M. V., & Kim, D. S. (2016). Adsorption of methyl orange from aqueous solution by aminated pumpkin seed powder: Kinetics, isotherms, and thermodynamic studies. *Ecotoxicology and Environmental Safety*, *128*(Supplement C), 109-117. doi:10.1016/j.ecoenv.2016.02.016.

Vargas, J. A., & Forero, A. H. (2011). Obtención de hierro a partir de arenas negras del Atlántico colombiano. Desembocadura río Magdalena. *Revista de la Facultad de Ingeniería*, *26*, 19-26.

Wang, E., Zheng, Q., Xu, S., & Li, D. (2011). Treatment of Methyl Orange by Photocatalysis Floating Bed. *Procedia Environmental Sciences*, *10*(Part B), 1136-1140. doi:10.1016/j.proenv.2011.09.181.

Yan, J., Zhu, Y., Qiu, F., Zhao, H., Yang, D., Wang, J., & Wen, W. (2016). Kinetic, isotherm and thermodynamic studies for removal of methyl orange using a novel β-cyclodextrin functionalized graphene oxide-isophorone diisocyanate composites. *Chemical Engineering Research and Design*, *106*(Supplement C), 168-177. doi:10.1016/j.cherd.2015.12.023